FUNCTIONALLY-GRADED SSIC/AA6082/HDPE COMPOSITE SHIELDS FOR MMOD HYPERVELOCITY IMPACT MITIGATION

KAYLEIGH MOORE & FILIPE TEIXEIRA-DIAS
Institute for Infrastructure and Environment (IIE), School of Engineering, University of Edinburgh, UK

ABSTRACT
Protecting low Earth orbit infrastructure from micrometeoroid and orbital debris impacts remains a critical challenge in modern space engineering. Traditional shielding systems often face challenges in balancing weight and impact resistance. This study explores an impedance-graded shielding approach, incorporating sintered silicon carbide (SSiC), aluminium alloy 6082 (AA6082) and high-density polyethylene (HDPE) to enhance hypervelocity impact mitigation. The combination of graded mechanical impedance and multiple material failure mechanisms within the system offers significant potential for minimising damage to space structures by enhancing projectile fragmentation and maximising energy dissipation. The smoothed particle hydrodynamics method was implemented to model a 4 mm diameter spherical AISI 304 projectile impacting multiple arrangements of AA6082, SSiC and HDPE at 5 km/s. The resulting debris cloud data was analysed to visually assess the performance of different configurations. The findings demonstrate that the graded structure significantly improves stress wave dispersion and reduces the kinetic energy of the impactor, providing insights for the design of next-generation spacecraft shielding systems.
Keywords: impedance-grading, hypervelocity impact, smoothed particle hydrodynamics, Whipple shield, debris cloud.

1 INTRODUCTION

The proliferation of artificial satellites and the increasing density of orbital debris have amplified the risk posed by micrometeoroid and orbital debris (MMOD) impacts, particularly in low Earth orbit (LEO). Traditional shielding solutions, such as the Whipple shield (Fig. 1), provide a degree of protection against hypervelocity impacts (HVI) by using a sacrificial front bumper plate to fragment incoming projectiles and generate a debris cloud, which then disperses its kinetic energy across a rear wall [1]. However, optimising these systems to maximise impact resistance while maintaining mass efficiency restraints remains an ongoing challenge.

Recent research has explored multi-material, impedance-graded shielding systems to address the limitations of traditional configurations. These systems employ layers of materials with varying mechanical impedance and distinct failure modes to enhance energy dissipation and promote projectile fragmentation under HVI conditions [3], [4]. The mismatch in mechanical impedance between adjacent material interfaces can result in an increase in peak shock pressure and pressure pulse duration when graded from high-to-low impedance due the wave interaction within each layer. This was demonstrated by Cherniaev and Telichev [3] using a ceramo-aluminium bumper with a SiC coating, and by Wen and Chen [4] using a layered shield composed of aluminium alloy, magnesium alloy, and steel. Zhang et al. [5] investigated a Ti6Al4V/AA2024-T4/PA66 shielding system under an impact velocity of 6.5 km/s. The graded metal–polymer configuration generated high shock pressures and elevated temperatures, contributing to increased projectile fragmentation. Additionally, the wave propagation path and duration were significantly influenced by the graded structure, allowing more time for temperature rise and material break-up. The extreme

WIT Transactions on The Built Environment, Vol 215, © 2025 WIT Press
www.witpress.com, ISSN 1743-3509 (on-line)
doi:10.2495/SUSI250221

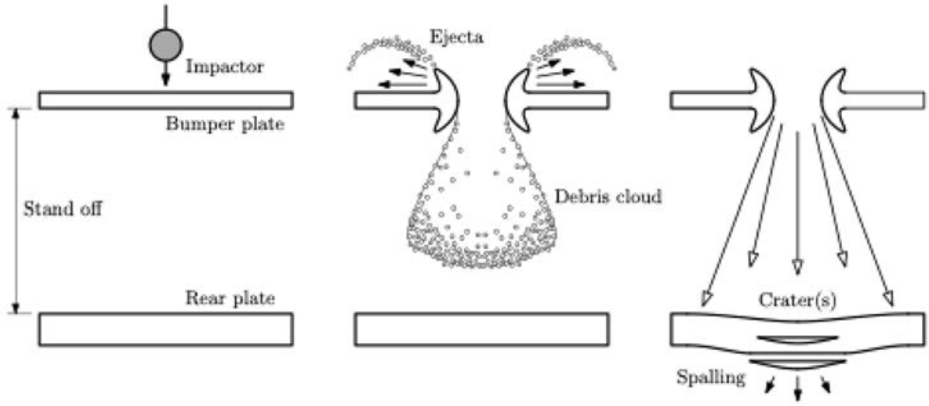

Figure 1: Whipple shield schematic. *(Source: Reprinted from Fowler and Teixeira-Dias [2], licensed under CC BY 4.0.)*

strain-rate response of high-density polyethylene (HDPE) under HVI has only recently been studied and modelled, by Rogers et al. [6]. While HDPE is likely unsuitable for standalone HVI protection, its low weight, cost-effectiveness, bulk melting capability, and capacity for large-scale plastic deformation suggest potential for its use within a layered shielding system.

This study investigates the potential of using sintered silicon carbide (SSiC), aluminium alloy 6082 (AA6082) and high-density polyethylene (HDPE) in combination to optimise projectile fragmentation and reduce residual kinetic energy, thereby enhancing overall protective performance. The proposed ceramic–metal–polymer configuration incorporates a high-impedance ceramic front layer to amplify shock pressure within the shield, a metallic layer to facilitate plastic deformation and a polymer backing layer to contribute to bulk melting and additional energy absorption through plastic deformation. While ceramic–metal systems have been widely studied and proven effective, the incorporation of HDPE in such multi-layered configurations remains largely unexplored.

2 MODELLING

A numerical model was developed, and the corresponding simulations were carried out in IMPETUS Afea using the surface smoothed particle hydrodynamics (SPH) solver for the target configurations listed in Table 1. The thickness of each layer was adjusted to maintain an approximately constant areal density across all configurations. An AISI 304 spherical projectile, 4 mm in diameter, was used in all simulations – except for the HDPE validation model discussed in Section 2.1 – impacting the target plates at a velocity of 5 km/s under normal incidence. The SSiC plate was modelled using the Johnson–Holmquist II (JH2) constitutive model to capture its dynamic brittle behaviour, alongside a polynomial equation of state (EoS). The AA6082 aluminium alloy was represented using the Johnson–Cook constitutive model, which incorporates work hardening, strain-rate sensitivity, and thermal softening, along with the Johnson–Cook damage model and the Grüneisen EoS.

HDPE was also modelled using the Johnson–Cook constitutive and damage models to account for its response under high strain rates. The material parameters for all constitutive models and equations of state are provided in Table 2. A particle density of approximately 10 particles/mm was used to ensure convergence, with negligible variation observed in the results.

Table 1: Target composition and thickness.

Layer configuration	**Thickness (mm) L_1/…/L_n**
AA6082	3.62
HDPE	11.00
SSiC/AA6082	1.50/2.30
SSiC/HDPE	1.50/6.00
SSiC/AA6082/HDPE	1.50/1.27/2.00

Table 2: Material properties for SSiC, AA6082 and HDPE.

		SSiC [7], [8]		AA6082 [9]	HDPE [10]	AISI 304 [11]–[13]
	ρ (kg/m^3)	3150	ρ (kg/m^3)	2700	954	7950
	G (GPa)	179.825	*G* (GPa)	26.923	0.276	75.391
Constitutive model	Johnson–Holmquist		Johnson–Cook			
	A	0.960	*A* (MPa)	250.00	31.27	310
	B	0.350	*B* (MPa)	243.60	0.00	1000
	C	0.009	*N*	0.17	0.75	0.65
	M	1.000	*C*	0.00747	0.04	0.07
	N	0.650	*M*	1.31	0.85	1
	σ_H (GPa)	11.70				
	T (GPa)	0.750				
Damage	Johnson–Holmquist		Johnson–Cook			
	D_1	0.48	D_1	0.0164	0.05	0.53
	D_2	0.48	D_2	2.2450	1.48	0.5
			D_3	−2.798	−1.50	−6.8
			D_4	0.007	0.25	0.014
			D_5	3.65	0.00	0
Equation of state	Polynomial		Mie–Grüneisen			
	K_1 (GPa)	220	γ_0	1.97	0.86	1.93
	K_2 (GPa)	361	S_1	1.339	7.9	1.49
	K_3 (GPa)	0	S_2	0.000	2.296	0
	β	1.0	S_3	0.000	43.36	0

2.1 Validation

To validate the material models used, monolithic HDPE targets were modelled using parameters consistent with the experimental work of Rogers et al. [6]. A comparison between the experimental results and the current numerical work is shown in Fig. 2. A strong correlation is observed in both debris cloud formation and ejecta geometries at impact velocities of 3.75 km/s and 5 km/s, confirming the validity of the numerical approach.

3 RESULTS AND DISCUSSION

The absolute values for target perforation, debris cloud velocity, and geometric characteristics are presented in Table 3. The maximum head velocity – measured at the tip of the debris cloud – is greater for the monolithic targets compared to the multi-layered

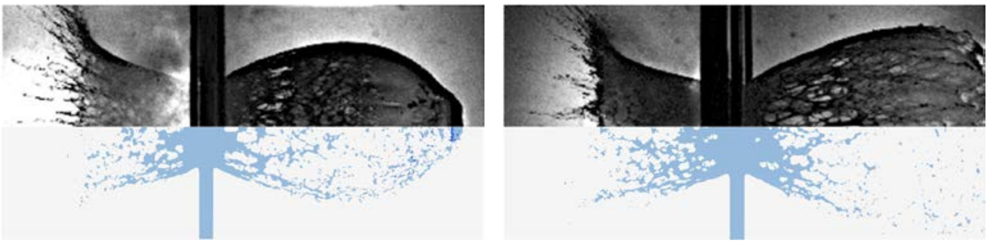

Figure 2: Experimental and numerical results of impact on HDPE target: at 3.75 km/s (left) and 5.00 km/s (right).

Table 3: Target composition and thickness.

Layer configuration	Perforation diameter (mm)	Max. head velocity (m/s)	Debris cloud dimensions at 30.4 μs		
			Angle, α (°)	Length, l (mm)	Height, h (mm)
AA6082	11.3	4,040.5	35	125.0	45
HDPE	26.7	3,811.4	9	118.6	61
SSiC/AA6082	8.6	3,589.7	41	103.3	64
SSiC/HDPE	30.6	3,554.3	15	100.0	56
SSiC/AA6082/HDPE	25.3	3,585.1	43	105.3	63

configurations. Similarly, the debris cloud length, measured from the rear surface of the target to the leading edge of the cloud, is also longer for both monolithic targets. These results indicate reduced effectiveness of the monolithic shields in dissipating impact energy and containing the debris cloud relative to the multi-layered systems.

The SSiC/HDPE target shows a slightly lower maximum head velocity compared to the SSiC/AA6082 and SSiC/AA6082/HDPE configurations; however, the difference among these three configurations is less than 1% (0.98% and 0.86%, respectively). This suggests that the front layer plays a more dominant role in influencing the residual velocity of the projectile than the rear layers. Notably, targets with HDPE as the rearmost layer display significantly larger perforation diameters than those with AA6082 in the same position. This indicates that HDPE may serve as a beneficial rear-layer material, likely due to its capacity for large-scale plastic deformation, which can contribute to increased material displacement and energy absorption.

An increase of 67% in debris cloud angle is observed when comparing the HDPE target to the SSiC/HDPE configuration, while a 17% increase is noted from the AA6082 target to the SSiC/AA6082 configuration. The addition of the high-impedance ceramic layer results in a greater spread of the debris cloud, particularly in the configurations incorporating HDPE.

The relative performance in terms of projectile residual kinetic energy and mass reduction is assessed by comparison with the monolithic AA6082 target, used as the baseline solution, as shown in Fig. 3. The monolithic HDPE target is excluded from this comparison, as it exhibited a residual kinetic energy 3.8 times greater than that of the AA6082 target, highlighting the unsuitability of monolithic HDPE as an effective shielding material under HVI conditions.

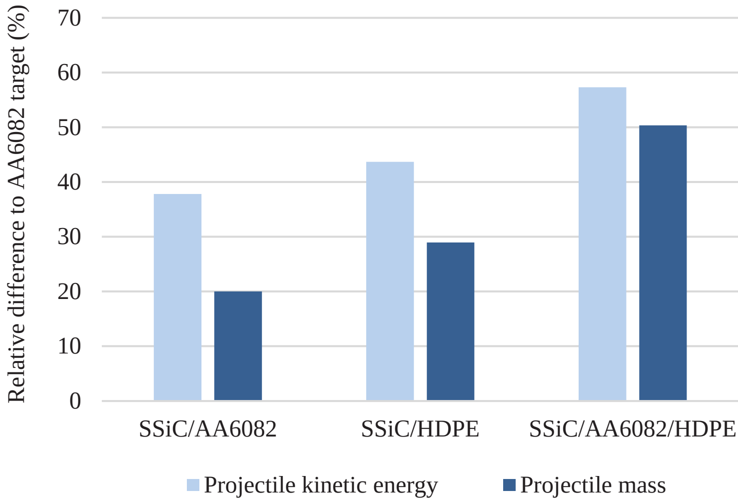

Figure 3: Relative difference of projectile kinetic energy and mass compared with AA6082 target.

The relative differences in projectile kinetic energy for the SSiC/AA6082, SSiC/HDPE, and SSiC/AA6082/HDPE target configurations are 37.8%, 43.7% and 57.3%, respectively. In terms of mass reduction, the SSiC/AA6082, SSiC/HDPE, and SSiC/AA6082/HDPE targets exhibit reductions of 20.0%, 29.0% and 50.4%, respectively, compared to the AA6082 baseline solution. Despite the poor performance of the monolithic HDPE target, the layered SSiC/HDPE configuration outperforms the SSiC/AA6082 configuration in both reducing projectile kinetic energy and mass loss, while maintaining the same target areal density. The SSiC/AA6082/HDPE shield further reduces both projectile kinetic energy and mass. These improvements can be attributed to the interaction of stress waves and the combined failure mechanisms within the layered structure, which enhance energy dissipation and material fragmentation.

4 CONCLUSION

Multiple target configurations comprising SSiC, AA6082, and HDPE components were modelled using SPH to evaluate their protective performance under HVI. Analysis of the resulting debris cloud data revealed that layered targets with an SSiC front layer provided enhanced protection compared to monolithic AA6082 and HDPE targets. The SSiC/AA6082/HDPE configuration demonstrated a 57.3% reduction in projectile residual kinetic energy and a 50.4% reduction in projectile mass relative to the AA6082 baseline solution. These findings highlight that, although monolithic HDPE shields are ineffective for HVI protection, the inclusion of HDPE within layered systems offers promising potential for the development of advanced passive protection solutions and requires further investigation.

ACKNOWLEDGEMENT

The authors acknowledge the support given to this project by the Engineering and Physical Sciences Research Council (EPSRC) (grant: EP/W524384/1).

REFERENCES

[1] Whipple, F., Meteoroid and space travel. *Astron. J.*, **1161**, p. 132, 1947.
[2] Fowler, K. & Teixeira-Dias, F., Optimisation of hybrid composite shields for hypervelocity micro-meteoroid and orbital debris (MMOD) impact. *Adv. Space Res.*, **73**(12), pp. 6194–6208, 2024.
[3] Cherniaev, A. & Telichev, I., Sacrificial bumpers with high-impedance ceramic coating for orbital debris shielding: A preliminary experimental and numerical study. *Int. J. Impact Eng.*, **119**, pp. 45–56, 2018.
[4] Wen, K. & Chen, X., Influence of the impedance gradient on the debris cloud produced by hypervelocity impact. *Int. J. Impact Eng.*, **159**, 104034, 2022.
[5] Zhang, P.L. et al., Study of the shielding performance of a Whipple shield enhanced by Ti-Al-nylon impedance-graded materials. *Int. J. Impact Eng.*, **124**, pp. 23–30, 2019.
[6] Rogers, J.A., Mead, P., Wilkerson, J., Lacy, T. & Williams, N., Hypervelocity impact response of monolithic UHMWPE and HDPE plates. *Int. J. Impact Eng.*, **161**, 104081, 2022.
[7] Liu, Y., Li, B., Wu, C. & Zheng, Y., Simulation-based evaluation of surface micro-cracks and fracture toughness in high-speed grinding of silicon carbide ceramics. *Int. J. Adv. Manuf. Technol.*, **86**, pp. 799–808, 2016.
[8] Saint-Gobain, Hexoloy® SA Silicon Carbide – Technical Data Sheet. www.ceramicsrefractories.saint-gobain.com/files/4731/view. Accessed on 8 Apr. 2025.
[9] Adeyinka, A.M. & Olaleke, M.O., Predictive model for thermal response during dry machining of Al 6082-T6 using FEM. *Int. J. Eng. Res.*, **9**(6), pp. 1261–1271, 2020.
[10] Mead, P., Rogers, J., Williams, N., Wilkerson, J. & Lacy, T., Simulating hypervelocity impacts to monolithic high-density polyethylene plates. 2023. https://doi.org/10.31224/3205.
[11] Zou, Z., He, L., Zhou, T., Zhang, W., Tian, P. & Zhou, X., Research on inverse identification of Johnson–Cook constitutive parameters for turning 304 stainless steel based on coupling simulation. *J. Mater. Res. Technol.*, **23**, pp. 2244–2262, 2023.
[12] Cai, S., Liu, J., Cheng, Y., Hao, W. & Zhang, P., Numerical investigation into the effect of stand-off distance on the blast performance of metallic corrugated-core sandwich panels. Presented at *ASME 2018 37th Int. Conf. Ocean, Offshore and Arctic Eng.*, American Society of Mechanical Engineers Digital Collection, 2018.
[13] Junxiang, Q., Guanghong, M., Jiuying, A. & Yu, H., Study on numerical simulation of TA1-304 stainless steel explosive welding. *China Weld.*, **30**(2), pp. 11–16, 2021.